

The effect of impeller type on the mixing time of the non-Newtonian fluids in stirred tanks

Hani Taleshi Ahangari*, Pariya Noeparvar, Jafar Sadegh Moghaddas

Sahand University of Technology, Transport Phenomena Research Center, Chemical Engineering Faculty, Tabriz, (IRAN)

E-mail: hanitaleshi@gmail.com; paria1219@gmail.com; jafar.moghaddas@sut.ac.ir

ABSTRACT

In the following paper, experimental data represent mixing time in a stirred tank. Electrical conductivity methods are used to obtain results of mixing time. Weight percent of CMC solution, which indicates pseudo plastic behavior of the fluid, was deemed 0.5%. What is more, it was used as continuous phase and air as the dispersed phase. The effect of blade angle and length were investigated with 7 concave impellers. The experimental results demonstrate that the mixing time will decrease by increasing rotation speed. The impeller No. 6 is favorable to reduce mixing time in constant power consumption because of the maximum angle between the other impellers. Consequently, an equation to predict mixing time by using four independent parameters is suggested; moreover, this equation can be utilized as a predictor relation in comparison with the experimental data.

© 2016 Trade Science Inc. - INDIA

KEYWORDS

Mixing time;
Concave impeller;
Speed;
Aeration;
Non-Newtonian fluids.

INTRODUCTION

Mixing is a combination of two or more different substances which results ideal homogeneous physical and chemical products. This is a technique used widely within industries such as paper, plastics, ceramics, foods, medicines and so forth^[1]. Mixing time is a significant determinant for phase mixtures as well as parameters in phenomena interpretation. The methods of mixing time measurement are divided in two groups: physical and chemical. The comparison of mixing time highly depends on the definitions, methods of measurement, non-homogeneous, types of probe and tools by which the tracer is injected and its location^[2]. An important part of industry products consists of non-Newtonian fluids

applied in food industries such as yoghurt and soup. Shear stress behaviors of these fluids are not investigable with the relations of Newtonian fluids; in other words it is difficult to predict interactions. The few available researches have focused on macroscopic aspects of the flow; therefore, research regarding fluid foundations is serious need in determining fluid properties (Rheology)^[3,4]. Stirred tanks are more applicable than any other mixer systems; furthermore, tanks with stirrers have the largest surface of contact and are the best facilities for mixing in non-Newtonian fluids^[5]. Mixers in the tanks create a series of cuts and flow lines in the liquids. Effects in transfer of momentum and layers of liquid movements in sections of the tank eventuate in combining of liquids into a single mixture^[6,7].

Full Paper

The power law shows the behavior of the pseudo plastic fluid (Eq. 1):

$$\tau = K\dot{\gamma}^n \quad (1)$$

Where τ , K , $\dot{\gamma}$ and n are shear stress, power law constant or consistency index, shear rate and power law exponent or flow behavior index, respectively. In which relates the shear stress in the fluid to the shear rate being exerted on it. Dynamic viscosity relation is indicated by Eq. 2:

$$\mu_A = \frac{\tau}{\dot{\gamma}} = K\dot{\gamma}^{n-1} \quad (2)$$

Where μ_A is apparent viscosity of the fluid^[8]. Bird et al. predict an equation for the shear rate on the wall of a baffled tank as a function of the torque on the mixer shaft as shown by Eq.3:

$$\Lambda = \mu \iint_S R \left(\frac{\partial v_\theta}{\partial r} \right)_w dS + \iint_A R p_{baff} dA \quad (3)$$

Where Λ , R , r , S , P_{baff} and A are torque on the shaft, tank radius, radius, wall area, pressure on the baffles and area of baffles, respectively. The shear stress on the wall in a tank can be estimated by assuming the constant shear rate on the wall and applying the appropriate integration limits followed by Eq. 4:

$$\tau_w = \frac{1}{1.622} \left[\frac{\Lambda}{T^3} - 0.0638\rho(\Delta V)^2 \right] \quad (4)$$

Where τ_w , T , ρ and V are shear stress at the wall, tank diameter, fluid density and tank volume, respectively. It is worth to note that the contribution of the pressure can be ignored compared to the torque. Thus the estimated shear stress on the wall is calculated by Eq. 5^[8]:

$$\tau_w = \frac{1}{1.622} \left(\frac{\Lambda}{T^3} \right) \quad (5)$$

By respecting Eq. 2, the Reynolds number should be considered by Eq. 6^[8-10]:

$$Re = \frac{\rho ND^2}{\mu} = \frac{\rho ND^2}{K\dot{\gamma}^{n-1}} \quad (6)$$

Where Re , N and D are Reynolds number, impeller rotational speed and impeller diameter, respectively.

If an analogy is used between the pressure loss characteristic of the Non-Newtonian fluid and the power characteristic of a stirrer, Eq. 7 is achieved^[3, 8, 9]:

$$Re = \left[\frac{N^{2-n} D^2 \rho}{K} \times 8 \left(\frac{n}{6n+2} \right)^n \right] \quad (7)$$

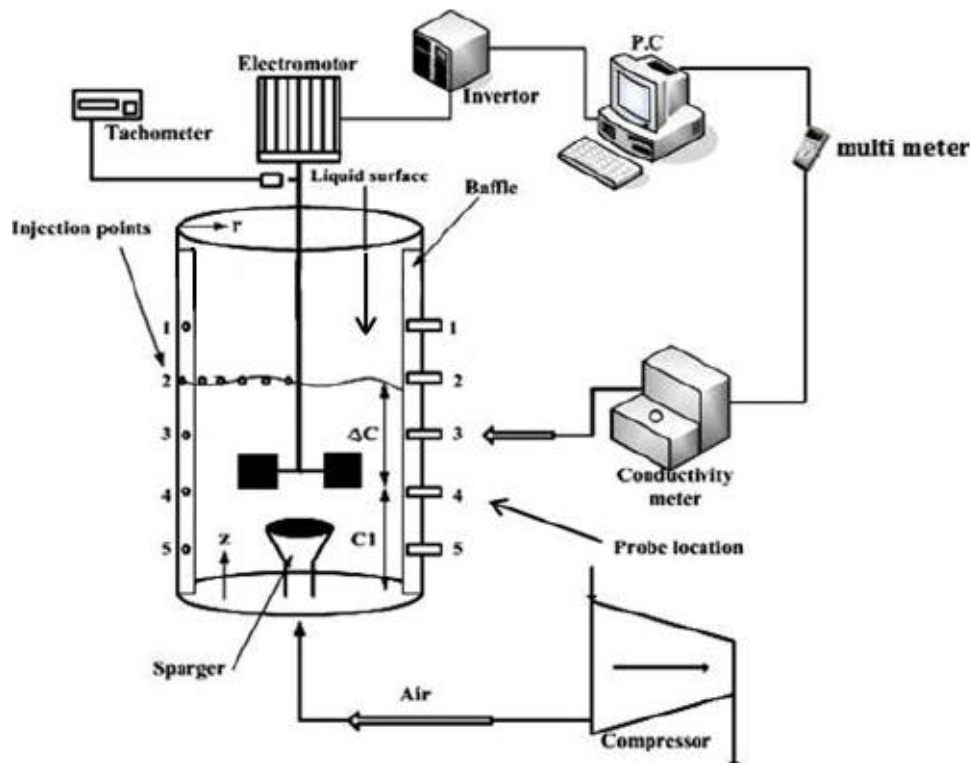


Figure 1 : Tank experimental system

Equipment and method

Geometric characteristics and experimental system of the tank are shown in Figure 1 and TABLE 1, respectively.

Figure 2 illustrates the shape of a concave impeller and the specifications of seven impellers are indicated by TABLE 2.

In the event of two phases, gas flow rate and distributed inside the liquid phase are measured by rotameter and gas sparger with the diameter of 7.5 cm with 31 holes each (1 mm diameter), respectively. The behavior of the non-Newtonian fluid can be determined by Rheometer; subsequently a shear stress is provided by exerting a shear rate on the solution. Based on these data, K and n in the Eq. 1 are achieved. TABLE 3 shows the results of Rheometer data in different weight percent solutions.

The aqueous solution in this research is of 0.5% in weigh of CMC. The 0.5% solution and measurements of viscosities include the values of $K=0.66$ and $n=0.66$ ^[5] 105.18 g of CMC should be solved in water based on of the stirred tank volume. A conductivity meter was used to measure mixing time and conductivity. A multi meter was also considered to change the electrical conductivity data to digital ones. 30 ml of saturated KCl solution was utilized as a tracer acted as a pulse at each step. The mixing time should be taken to inject the tracer until the contents of the tank reaches the favored degree of homogeneous is recorded. The degree of homogeneous is explained by the Eq. 8:

$$Y = |(C_i - C_0) / (C_\infty - C_0)| \quad (8)$$

Where C_i , C_0 , C_∞ and Y are initial, final, moment concentration of bulk mixture and degree of unifor-

TABLE 1 : Tank geometric characteristics

Geometric characteristics	
30Cm	Tank internal diameter (T)
30Cm	Liquid height (H)
3/T	Agitator diameter (D)
10/T	Baffles width (B)
100 T	Baffles thickness (h)
0.5 T	Distance between agitator and bottom of tank (C_1)
0.5 T	Distance between agitator and liquid level (ΔC)
-	Distance between two agitator (ΔC)
-	Distance between upper agitator and liquid surface (C_2)
-	Distance between lower agitator and liquid surface (C_1)



Figure 2 : Shape of a concave impeller

Full Paper

TABLE 2 : specifications of seven impellers (m)

	Impeller 1	Impeller 2	Impeller 3	Impeller 4	Impeller 5	Impeller 6	Impeller 7
Blade height (w)	0.025	0.025	0.025	0.0125	0.0375	0.050	0.025
Differences between blades (B-C)	0.00375	0.00625	0.0125	0.00625	0.00625	0	0
Blades angle (Degree)	40	40	40	25	50	55	40
Blades thickness(t)	0.002	0.002	0.002	0.002	0.002	0.002	0.002
Impeller diameter (D)	0.1	0.1	0.1	0.1	0.1	0.1	0.1

TABLE 3 : Samples of rheology results [4]

0.4 wt%		0.5 wt%		0.6 wt%		0.7 wt%	
Shear stress (pa)	Shear Rate (1/s)						
3.63	75	4.13	50	4.79	40	7.15	40
3.8	80	4.7	60	5.64	50	8.57	50
3.97	85	5.29	70	6.5	60	9.72	60
4.13	90	5.84	80	7.23	70	10.8	70
4.29	95	6.35	90	7.92	80	11.9	80
4.44	100	6.85	100	8.56	90	12.8	90
5.95	150	8.92	150	9.19	100	13.8	100
7.45	200	10.9	200	14.6	200	20.8	200
10.2	300	14.4	300	18.9	300	25.8	300
12.6	400	17.5	400	22.5	400	29.3	400
14.9	500	20.3	500	25.8	500	33.2	500
17	600	23	600	28.8	600	37	600
19	700	25.4	700	31.6	700	40	700
20.9	800	27.5	800	34.5	800	43.7	800
23.2	900	29.5	900	37.2	900	46.8	900
25.2	1000	32.1	1000	39.7	1000	49.8	1000
27.2	1100	34.3	1100	42	1100	52.8	1100
29.1	1200	36.3	1200	44.3	1200	55.7	1200
30.8	1290	37.9	1290	46.4	1290	58.1	1290
k= 0.14		k= 0.66		k= 0.90		k= 1.01	
n= 0.75		n= 0.66		n= 0.64		n= 0.58	

mity, respectively. Reaching the proper mixing, for instance, $Y=1$ in a limit time is almost impossible. A favored degree of uniformity is in the range of $Y=0.9-0.99$, and hence there are various explanations of mixing time due to this^[10, 11]. In this experiment the degree of homogeneity for mixing time is equal to $Y=0.95$.

RESULTS AND DISCUSSION

Effect of rotation speed

Reynolds number, torque on the shaft, shear stress on the wall and shear rate were shown in the TABLE

4 according to the used fluid, speeds and related equations.

At first, the effect of rotation speed on mixing time was examined for each of the 7 impellers. The rotation speeds of 200 and 400 and 600 rpm were tested in this study. As shown in Figures 3, 4 and 5, the mixing times for the impellers were measured at different gas flow rate.

It can be depicted that high rotation speeds is directly responsible for short mixing time in all cases. Rotational speed increases the power consumption, causing the increase of stress rates. The increase in shear stress is independent to the type of

TABLE 4 : Reynolds number at different speed for the 0.5 weight percent solution

N(rpm)	N(rps)	Re	Λ	τ_w	γ_w
100	1.66	69.5	5.326	121.592	2706.2
200	3.33	175.57	21.434	489.33	22313.7
300	5	301.7	48.325	1103.259	76477
400	6.66	441.4	85.739	1957.42	182313
500	8.33	594.4	134.128	3062.14	359148
600	10	757.9	193.3	4413	624802

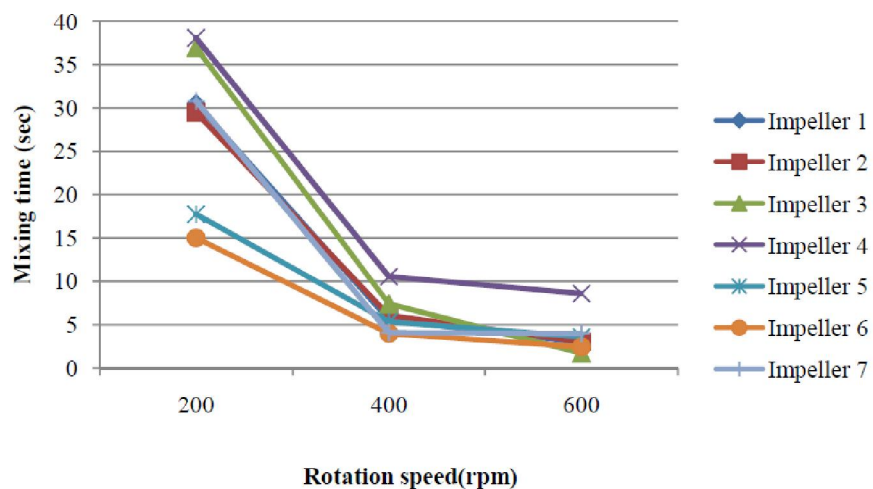


Figure 3 : Mixing time versus rotation speed for 7 impellers at Q=0 lit/hr

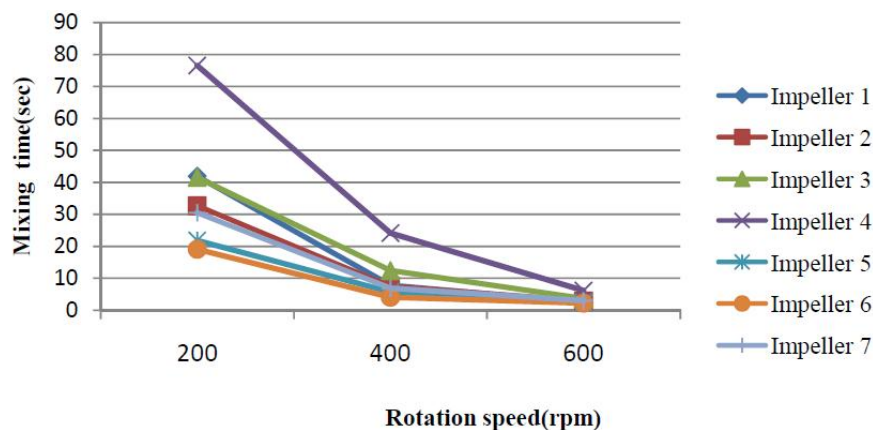


Figure 4 : Mixing time versus rotation speed at Q=100 lit/hr

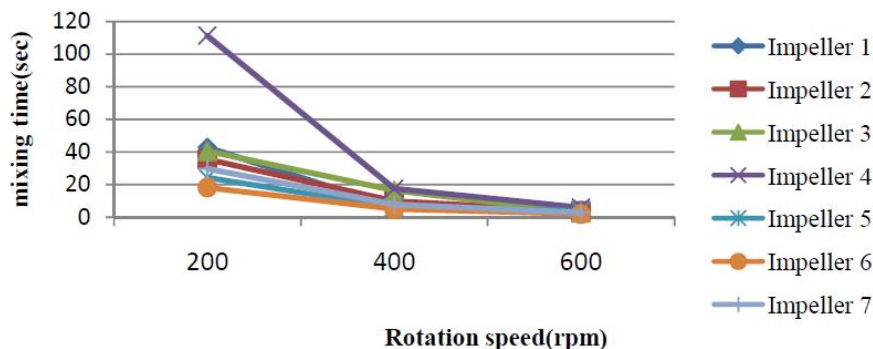


Figure 5 : Mixing time versus rotation speed at Q=200 lit/hr

Full Paper

impeller and causes to lead the rotation of the fluid in axial and radial directions.

Flow convection increases the Kinetic Energy of Eddy resulting in mixing time decrease. Mixing time, in terms of velocity, have a sharp slope at first and then decrease, so that at the speeds of 600 rpm and higher. The mixing time was not significantly different and power consumption will increase independently at this operation speed, subsequently, the fluid will behave as Newtonian fluids. It was observed that the impellers numbers 1, 2 and 7 will have the same result because of their equal blade height, angle; moreover, slight difference between them is due to the values in different blades for all rotation speeds. The impeller number 3 has the maximum blade difference but its blade height and angle is the same with impeller numbers 1 and 2, so the blade difference only causes to mixing time becoming longer. The impeller numbers 5 and especially 6 have the minimal mixing time in the constant power consumption due to the maximum angle and height between the blades. These impellers pump a higher flow in a rotation, thereby creating holes in the back of the blades. This causes the rotation speeds therefore increase whilst mixing time decreased. Hence it was clear that with increasing the rotation speed, mixing time was almost equal to that obtained by different impellers and is almost independent of the type of impeller.

Effect of aeration

As gas is a dispersed phase, the effect of gas on mixing time is expressed in terms of gas flow rate. Effects of aeration on mixing time at the speeds of

200, 400 and 600 rpm are shown for each of the individual impellers in Figures 6, 7 and 8.

At the presence of gas phase, different results occurred due to the complexity of two phase systems and the effects of various parameters on the distribution of bubbles. One of these parameters is the preferable impeller which was tested in this study. In general, the effect of aeration on mixing time changes in 4 cases as below.

1. Mixing time initially increased, and then decreased with aeration.
2. Mixing time increases with aeration.
3. Mixing time initially decreased and then increased with aeration.
4. Mixing time is independent of aeration.

As a rule of thumb it can be concluded that the first case occurs when the impeller is unable to effect the gas distribution and causes the impeller power to reduce. There is a critical value for this situation which after this, aeration helps the mixing (for example impellers No.2 and No.3). The second case is a subset of the first one which the impeller operates weaker in gas distribution or disturbance is not to that much that gas distribution is effective (for example impeller No.4). The third case occurs for the impellers which are larger in size because they reach to a maximum pneumatic mix suddenly (for example impellers No.5 and No.6). The fourth case depends on the operating conditions and such a situation is usually observed at high speeds.

The existence of gas phase in one hand causes the increase of pneumatic mixing in the system. That leads to shorter mixing time, but on the other hand mechanical mixing can be reduced by gas, resulting

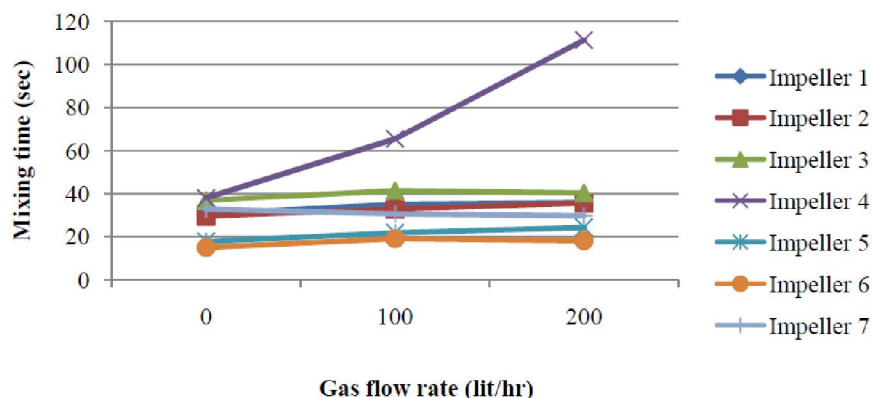


Figure 6 : Mixing time versus gas flow rate at 200 rpm

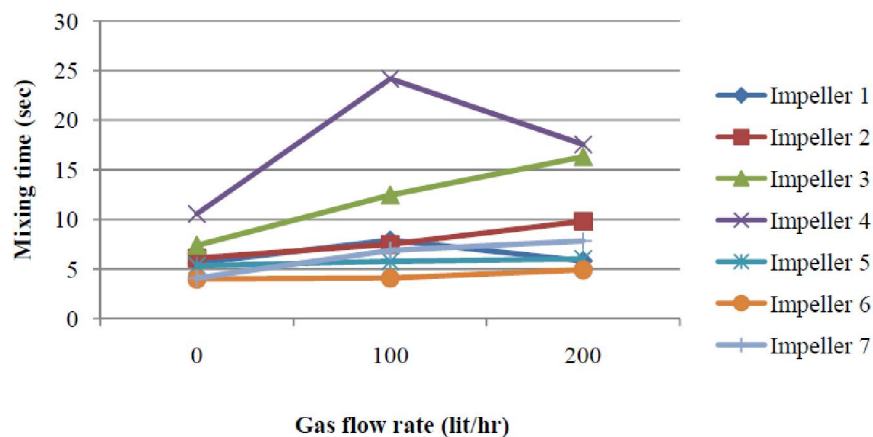


Figure 7 : Mixing time versus gas flow rate at 400 rpm

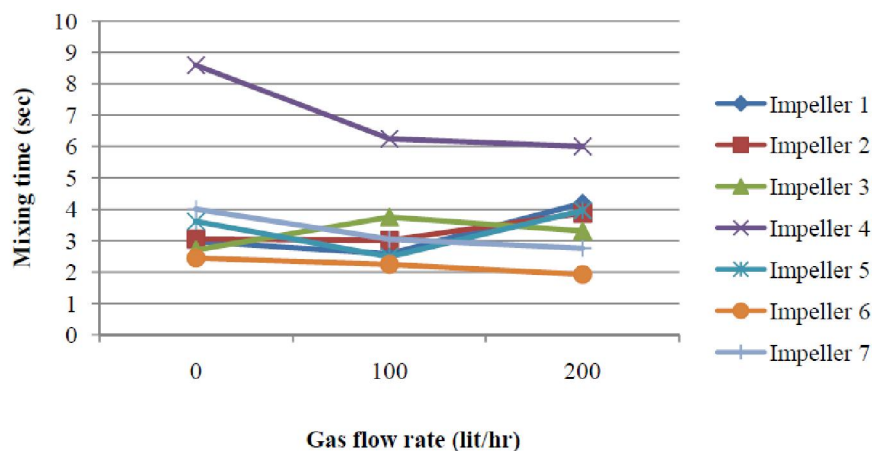


Figure 8 : Mixing time versus gas flow rate at 600 rpm

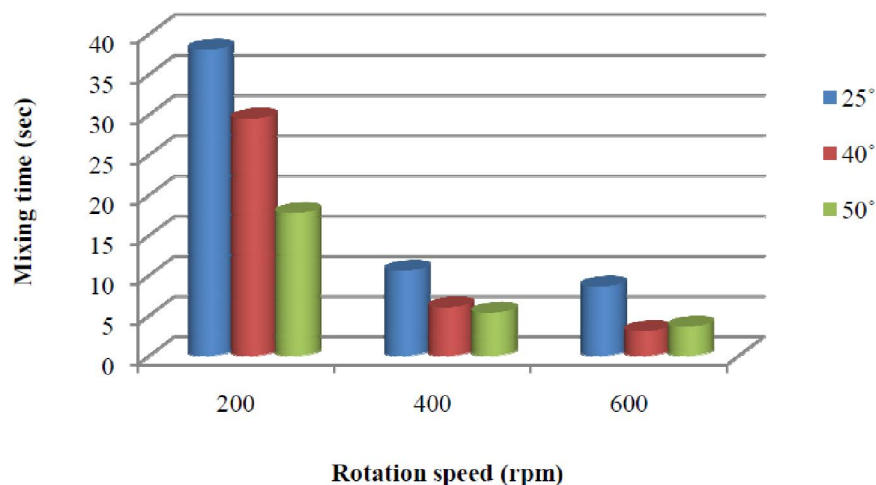


Figure 9 : Effect of blade angle on mixing time

in a higher mixing time. It is important to realize that the two factors are most effective at any test. Therefore, a different trend is observed for each impeller at any speed. At low speeds, the impeller No. 4 is weak in the gas distribution. A major part of bubbles reduce the mechanical mixing power without break-

ing by impeller and reach to the liquid surface. By increasing the speed to 600 rpm, it was found that the gas flow rate has little effect on mixing time. At medium to high speeds due to the prominent role of the rotation speed in creating turbulence flow, the gas flow rate does not significantly reduce mixing time.

Full Paper

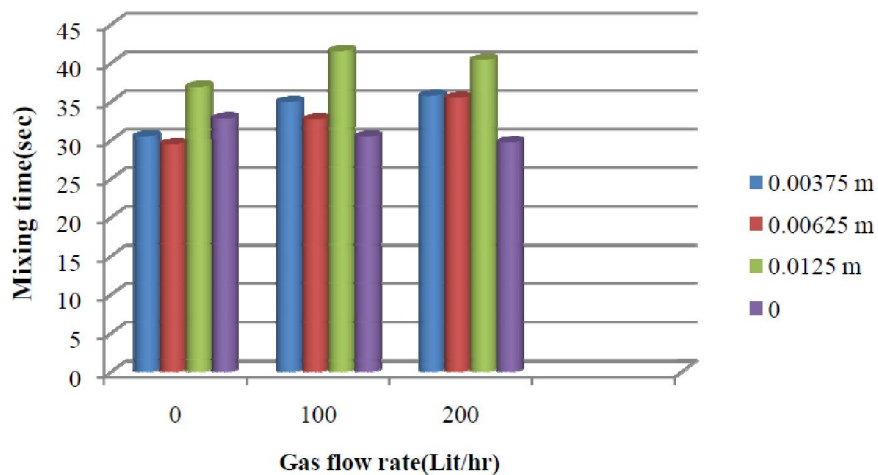


Figure 10 : Blade length effects on mixing time in different aerated intensity

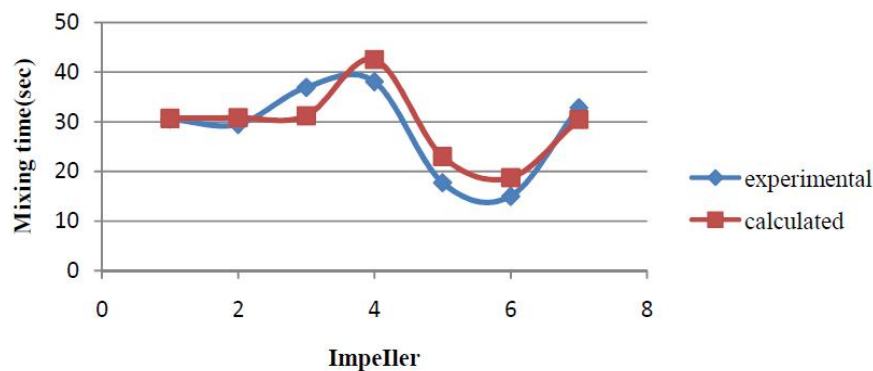


Figure 11 : Experimental and calculated mixing time at 200 rpm

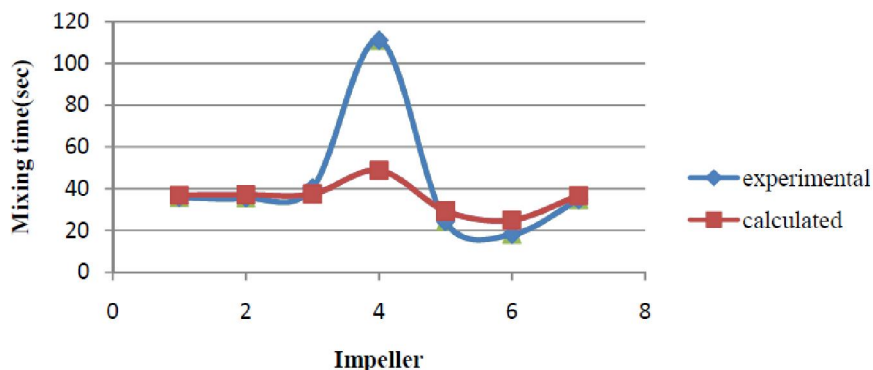


Figure 12 : Experimental and calculated mixing time in presence of gas at 200 rpm

EFFECT OF GEOMETRY

Blade angel

The effect of blade angle on mixing time is shown in Figure 9 for 25, 40 and 50 degrees.

For each of the cases, by increasing the blade angle, the flow number will rise and the impeller pumps increase flow to the rotation; consequently, homogeneity is obtained earlier and mixing time be-

comes shorter. By increasing the rotation speed, effects of blade angel decrease and nearly for all impellers, one mixing time was obtained.

Blade length

The effects of blade length on mixing time at different aeration rate, for the angle of 40 degrees and the speed of 200 rpm is shown in Figure 10. It can be illustrated that with increasing the blade length, the ability of impellers for breaking bubbles are reduced.

These bubbles decrease the impellers mechanical power without participating in flow patterns.

sult between them and Eq. 9 is appropriate for predicting mixing time.

CALCULATING MIXING TIME

According to the experimental data and linear regressions, calculating mixing time is suggested based on Eq. 9:

$$t = 150 \times \left[0.281 - \left(0.221 \times \left(\frac{N-200}{400} \right) \right) - \left(0.156 \times \left(\frac{\theta-25}{30} \right) \right) + (0.04 \times L) + \left(\frac{0.042 \times Q}{200} \right) \right] \quad (9)$$

Where t , θ , L and Q are mixing time, blade angle, blade length and gas flow rate, respectively.

Figures 11 and 12 depict the difference between experimental mixing time and calculated mixing time.

CONCLUSIONS

In this research the gas-liquid macro mixing in a stirred tank of specific geometry has been investigated with solution of 0.5% in weigh of CMC as the continuous phase and air as the dispersed phases with 7 different concave impellers. The mixing time has been determined by means of electrical conductivity method. The following findings were concluded:

The most efficient factor in reducing the mixing time is the rotation speed that by increasing dead zones which are affected by circulation will be lost and homogeneity occurs earlier and mixing time gets shorter. It occurred for all 7 impellers. Decreasing mixing time with increasing rotation speed was fast at first but then the curve grew less steep.

Increasing the rotation speed will also increase the power consumptions. In this study by respecting these factors the best speed is between 400 and 600 rpm.

The type of impeller is the most important factor in a constant power consumption that can reduce the mixing time. Because of the maximum blade angle and height, the impeller number 6 is the best and impeller number 4 is the worst.

Existence of gas phase has different effects on mixing time that depends on the parameters such as rotation speed, kind of impeller and the gas flow rate.

Calculated mixing time compared with the experimental data shows that there is acceptable re-

ACKNOWLEDGMENT

The authors would like to thank the technical staffs of Sahand University of Technology.

FUNDING

Transport Phenomena Research Center and the management of Sahand University of Technology are the funding sources for this project.

NOMENCLATURE

τ	shear stress, $\frac{N}{m^2}$
K	power law constant or consistency index, $pa \cdot s^n$
$\dot{\gamma}$	shear rate, s^{-1}
μ_A	apparent viscosity, pa. s
Λ	torque on the shaft, N.m
R	tank radius, m
S	wall area, m^2
P_{buff}	pressure on the baffles, pa
A	area of baffles, m^2
τ_w	shear stress at the wall, $\frac{N}{m^2}$
T	tank diameter, m
ρ	fluid density, $\frac{Kg}{m^3}$
V	tank volume, m^3
D	impeller diameter, m
C_i	initial concentration of bulk mixture, $\frac{mol}{lit}$
C_0	moment concentration of bulk mixture, $\frac{mol}{lit}$
C_∞	final concentration of bulk mixture, $\frac{mol}{lit}$
t	mixing time, sec
θ	blade angle, degree
L	blade length, m
Q	gas flow rate, $\frac{lit}{hr}$
Re	Reynolds number
N	impeller rotational speed, rpm
n	power law exponent or flow behavior index

REFERENCES

- [1] F.A.Holland, R.Bragg; "Fluid flow for chemical engineers", Edward Arnold, London, (1973).
- [2] L.Manna; "Comparison between physical and chemical methods for the measurement of mixing times", "Chem.Eng.Journal, DOI: 10.1016/S1385-8947(97)00059-4, **67(7)**, 167-173 (1997).
- [3] R.P.Chhabra, J.F.Richardson; "Non-newtonian flow in the process industries", Butterworth-Heinemann, ISBN: 978-0-7506-3770-1, (1999).
- [4] P.E.Arratia, T.Shinbrot, M.M.Alvarez, F.J.Muzzio; "Mixing of non-newtonian fluids in steadily forced systems", Physical Review Letters, DOI: 10.1103/PhysRevLett.94.084501, **94**, 1-3 (2005).
- [5] J.Eghbali; "A mixing study of non-Newtonian fluids in stirred tanks", M.Sc.thesis, Sahand University of Technology, Tabriz, Iran, (2011).
- [6] M.Zlokarnik; "Stirring: theory and practice", Wiley-VCH Verlag GmbH, (2001).
- [7] G.Ascanio, B.Castro, E.Galino; "Measurement of power consumption in stirred vessels", A-Review, Chem.Eng.Res.and Des., DOI: 10.1205/cerd.82.9.1282.44164, **82(9)**, 1282-1290 (2002).
- [8] E.L.Paul, Atiemo A.Obeng, S.M.Kresta; "Handbook of industrial mixing, science and practice", ISBN, 978-0-471-26919-9 (2004).
- [9] M.Zlokarnik; "Stirring : Theory and Practice", DOI: 10.1002/9783527612703.ch01, (2001).
- [10] Q.Zhang, Y.Yong, Z.S.Mao, C.Yang, C.Zhao; "Experimental determination and numerical simulation of mixing time in a gas-liquid stirred tank", Chem.Eng.Sci., DOI: 10.1016/j.ces.2009.03.030, **64(12)**, 2926-2933 (2009).
- [11] V.Roussinova, S.M.Kresta; "Comparison of continuous blend time and residence time distribution models for a stirred tank", J.Ind.Eng.Chem.Res., **47(10)**, 3532-3539 (2008).